J. Phys.: Theor. Appl. Vol. 10 No. 1 (2026) 36-43 doi: 10.20961/jphystheor-appl.v10i1.114433

Phase transformation in Fe–Ti–O composites as potential lead-free piezoelectric materials for energy sensor applications

Aulya Rizqi[1], Agus Yulianto[2], Budi Astuti[3]

[1,2,3] Physics Study Program, Faculty of Mathematics and Natural Sciences,
Semarang State University, Indonesia

Email: yulianto566@mail.unnes.ac.id

Received 11 January 2026, Revised 24 February 2026, Published 31 March 2026

Abstract: The Fe_2O_3–TiO_2 composite sintered at 900 °C exhibits a phase transformation from Fe_3O_4 to Fe_2O_3, which significantly affects the functional properties of the material. Composition variations (0:100 to 90:10) result in clear differences in densification, porosity, resistivity, and piezoelectric response. An increase in the Fe_2O_3 fraction strengthens densification but decreases piezoelectric voltage due to limited dipole movement. In contrast, the dominance of TiO_2 favors high resistivity while producing a maximum voltage of 0.01 V at a 10:90 composition. These results confirm that the balance of the Fe_2O_3–TiO_2 ratio determines the optimal combination of properties, as well as underscore the potential of this composite as an environmentally friendly lead-free piezoelectric material for sensor and energy device applications.

Keyword: Fe_2O_3–TiO_2; Densification; Piezoelectric; Sintering

1. Introduction

Metal oxide–based ceramic materials have attracted significant attention due to their ability to respond to electric fields, mechanical stress, and light (Hasan et al., 2022). Piezoelectric materials are of particular interest because they can reversibly convert mechanical energy into electrical energy (Anandakrishnan et al., 2023). Despite rapid market growth, most commercial piezoelectric devices still rely on lead-based PZT, raising environmental and health concerns (Prasetyo & Pradistia, 2022). Consequently, the development of environmentally friendly, lead-free piezoelectric materials has become an important research focus (Shen, 2025).

The Fe–Ti–O oxide system is promising because it combines the magnetic properties of Fe_3O_4 with the dielectric characteristics of TiO_2 (Jarollahi et al., 2023). Fe_3O_4 provides magnetic functionality, while TiO_2 offers chemical stability and high polarizability (Anucha et al., 2022). This combination enables multifunctional materials suitable for energy sensor applications (Kubiak, 2023).

Indonesia possesses abundant iron sand and TiO_2 resources, making the Fe–Ti–O system economically feasible for local material development (Kustiningsih et al., 2022).

However, high-temperature sintering may induce the transformation of Fe_3O_4 into Fe_2O_3, which can degrade magnetic stability and piezoelectric performance (Bora et al., 2011).

Previous studies have demonstrated high functional performance of Fe_3O_4–TiO_2-based composites in related applications (Gunlazuardi et al., 2021). Nevertheless, studies that specifically examine the relationship between phase transformation and piezoelectric response remain limited (Pap et al., 2025). Therefore, this study investigates the effect of Fe_3O_4–TiO_2 mass variation on phase transformation and its correlation with density, porosity, resistivity, and piezoelectric response.

2. Method

This study employed an experimental method with a quantitative approach. The primary materials were Fe_3O_4 powder (98% purity, 325 mesh) and TiO_2 powder (150 mesh), with a 5% polyvinyl alcohol (PVA) solution used as a binder. The Fe_3O_4–TiO_2 mass composition was varied to evaluate its effect on the physical and piezoelectric properties of the composites, following the oxide mixture approach proposed by Lubis and Daulay (2025). The detailed compositions are presented in Table 1..

Table 1 Composition of Research Materials

Experiment	Fe_3O_4 (gram)	TiO_2 (grams)
1	0	20
2	2	18
3	6	14
4	10	10
5	14	6
6	18	2

The Fe_3O_4 and TiO_2 powders were sieved, mixed with a PVA binder, dried at 100 °C for 30 minutes, and pressed into pellets at 3–4 tons (Taufik et al., 2011; Dewi et al., 2021). The pellets were sintered at 900 °C for 2 hours and naturally cooled to room temperature (Ghufron et al., 2020).

Phase composition was analyzed by X-ray diffraction using JCPDS 19-0629 (Fe_3O_4) and JCPDS 33-0664 (Fe_2O_3) as references (Pap et al., 2025). Piezoelectric output voltage was measured under periodic mechanical loading using aluminum-coated pellets, while electrical resistance was evaluated under dry and wet conditions (Rizky et al., 2023; Pranata et al., 2022).

Density, porosity, resistivity, and piezoelectric voltage were evaluated using Equations (1)–(3), and their relationships with compositional variation were analyzed by simple linear regression (Riani, 2023). All measurements were conducted at controlled room temperature and humidity..

$$\boldsymbol{\rho = \frac{m}{v}} \tag{1}$$

$$P = \left(1 - \frac{\rho_{eksperimen}}{\rho_{teori}}\right) x100\% \quad (2)$$

$$\boldsymbol{\rho = R\frac{A}{L}} \quad (3)$$

3. Results and Discussion

3.1. XRD Features

The X-ray diffraction (XRD) pattern of the Fe_3O_4–TiO_2 composite shows phase changes influenced by the composition ratio and sintering temperature. The characteristic peaks of Fe_3O_4 at approximately 30.1°, 35.5°, and 43.1° gradually weakened, while new peaks appeared at around 33.2°, 35.6°, and 54.1°, indicating the formation of Fe_2O_3 (Pap et al., 2025). This transformation agrees with the report by Ghufron et al. (2011), which states that the oxidation of Fe_3O_4 to Fe_2O_3 occurs due to oxygen diffusion at elevated temperatures. The color change of the samples from black to reddish-brown further confirms the formation of hematite during the sintering process. TiO_2 peaks at around 25.3° remained visible, indicating that the anatase phase was stable up to 1000 °C. This phase shift is closely related to the densification process, which affects the density and porosity of the composite. The gradual replacement of Fe_3O_4 by Fe_2O_3 enhances the microstructural integrity and promotes improved particle connectivity within the sintered body.

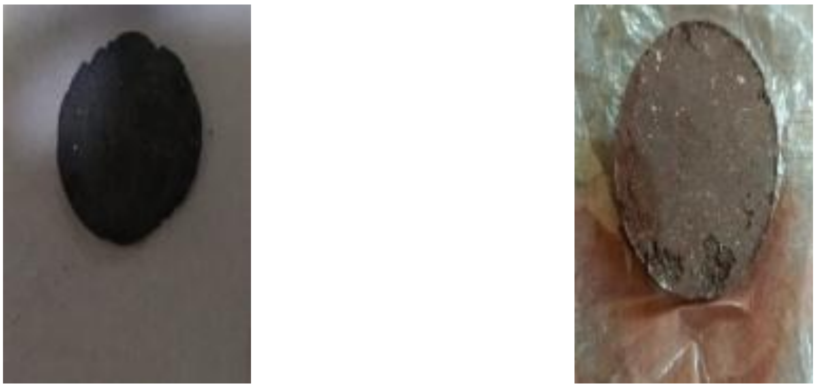

(a) Before sintering (b) After sintering

Figure 1 Color of Fe_3O_4–TiO_2 composite samples before and after sintering at 1000°C

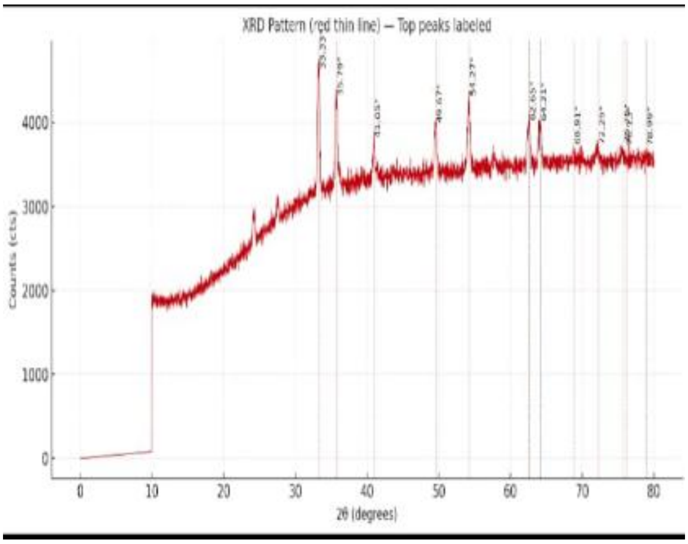

Figure 2 XRD pattern

3.2. Microstructure: Density and Porosity

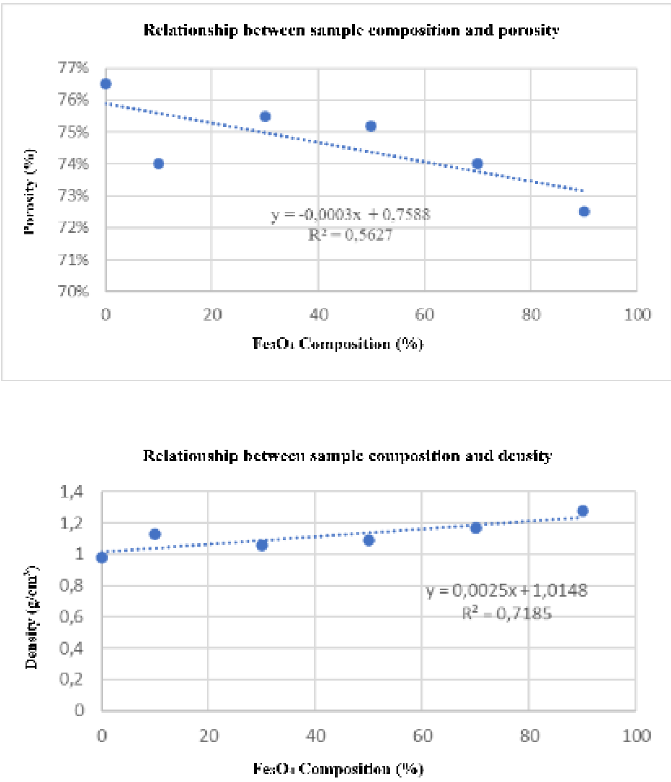

Figure 3. Relationship between Fe_3O_4 TiO_2 composition and Microstructure.

The phase transformation observed in the XRD results significantly increased the material density from 0.98 g·cm⁻³ to 1.28 g·cm⁻³, indicating effective sintering and improved grain connectivity (Waruwu, 2023). Concurrently, porosity decreased from 76.7% to 72.5%, reflecting enhanced densification driven by Fe-ion diffusion during sintering (Khlyustova et al., 2020). These results demonstrate that the Fe_3O_4–TiO_2

composition strongly influences the microstructure by regulating density and porosity. A denser microstructure improves grain contact and reduces charge trapping, thereby enhancing the piezoelectric response (Roscow et al., 2016)

3.3. Electrical Properties: Dry and Wet Resivitability

Improvements in the microstructure due to increased density significantly affected the resistivity values of the composites. The dry resistivity decreased from 31.42 kΩ to 14.38 kΩ, while under wet conditions it ranged from 24.0 to 7.37 kΩ

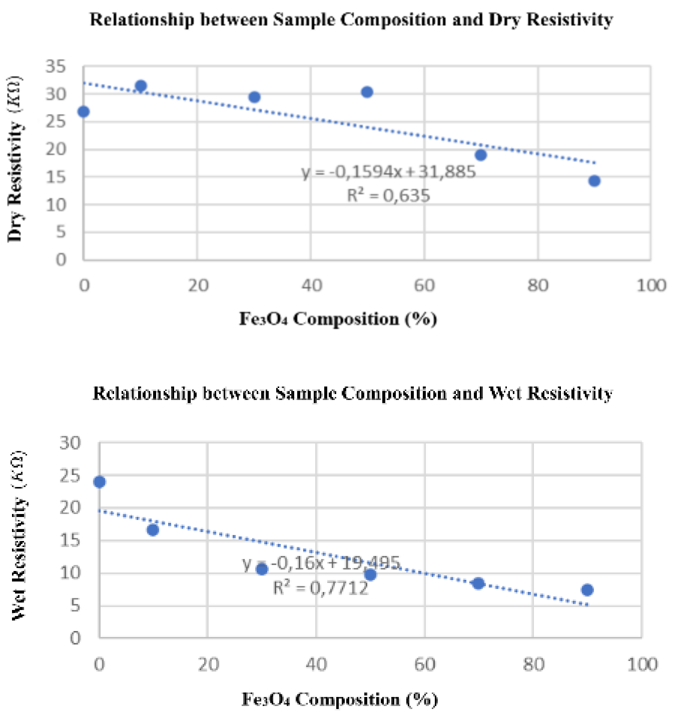

Figure 4 Variation in the resistivity of Fe_3O_4–TiO_2 composites

This decrease indicates an enhancement of conduction pathways facilitated by the Fe^{2+}/Fe^{3+} electron hopping mechanism. Lower resistivity in wet conditions is attributed to the contribution of ionic conduction within the pores, where moisture acts as a charge carrier medium. The R^2 value under wet conditions demonstrates a consistent influence of composition on conductivity. These results are consistent with the increased density and Fe_2O_3 formation, both of which expand the charge transport pathways within the composites.This finding is in good agreement with the results reported by Lumban Toruan et al. (2023), who stated that water can enhance the ionic conductivity of porous materials. The correlation between composition, microstructure, and resistivity thus confirms the crucial role of Fe-ion diffusion and porosity reduction in improving electrical performance.

3.4. Piezoelectric Response: Output Voltage

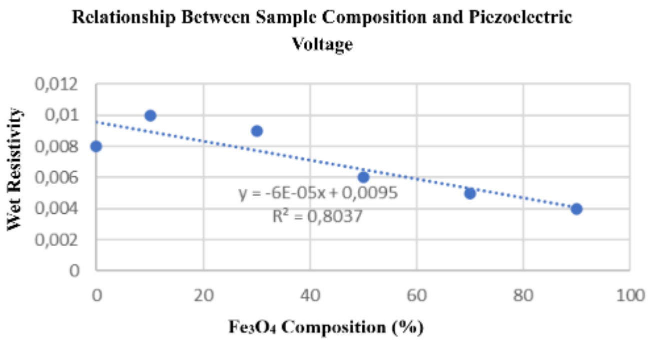

Figure 5 Piezoelectric voltage to Fe_3O_4–TiO_2 composition ratio.

Phase transformation induced changes in conductivity and density significantly affected the piezoelectric output voltage. The highest voltage was obtained at a Fe_3O_4–TiO_2 ratio of 10:90, where the TiO_2-dominant composition provided an optimal balance between conductivity and dielectric constant, enabling efficient charge accumulation at the electrode interfaces. In contrast, increased Fe_2O_3 content reduced the output voltage due to charge relaxation and restricted dipole movement (Limbong, 2013). The relatively low R^2 value indicates that phase distribution and microstructural heterogeneity also influence energy conversion efficiency (Yotthuan et al., 2018). Overall, controlling the Fe/Ti ratio is critical for optimizing dipole alignment, charge transport, and electromechanical response in Fe–Ti–O composites.

4. Conclusion

Variations in the Fe_2O_3–TiO_2 composition significantly affect the density, porosity, resistivity, and piezoelectric voltage of the composite. Increasing the Fe_2O_3 fraction enhances densification and reduces porosity, while a higher TiO_2 fraction yields the maximum piezoelectric voltage of 0.01 V at a 10:90 composition ratio. Therefore, the Fe_2O_3–TiO_2 system demonstrates strong potential as a lead-free, metal oxide–based piezoelectric material for sensor and energy-harvesting applications. These findings provide a valuable reference for developing environmentally friendly piezoelectric ceramics utilizing locally sourced raw materials.

References

Anandakrishnan, V., Muralidharan, R., & Dhanalakshmi, S. (2023). Toward ecofriendly piezoelectric ceramics—Reduction of lead-based ceramics through compositional design and sintering optimization. *Materials Today: Proceedings*, *72*, 215–223.

Anucha, C., Limphirat, W., & Suwanboon, S. (2022). Phase transformation and dielectric behavior of TiO_2 ceramics. *Journal of Materials Science*, *57*(12), 9854–9866.

Bora, T., Sathe, B. R., & Dutta, J. (2011). Defect-mediated charge transport in Fe_2O_3 for photocatalysis. *Catalysis Today*, *161*(1), 14–20.

Ghufron, M., Kusumaatmaja, A., & Siregar, H. (2011). Fe_3O_4 phase transformation to

Fe_2O_3 in the high-temperature sintering process. *Indonesian Journal of Physics*, *15*(2), 33–39.

Ghufron, M., Lestari, A., & Wibowo, T. (2020). The effect of high temperature on the structure of iron oxide. *Ceramics Research Journal*, *14*(2), 102–110.

Gunlazuardi, J. et.al. (2021). Magnetic separation and photocatalytic performance of $Fe_3O_4/SiO_2/TiO_2$ composite. *Makara Journal of Science*, *25*(4), 236–246.

Hasan, M. A., Pap, Z., & Baia, L. (2022). Fe_3O_4–Ag/TiO_2 nanocomposites for enhanced wastewater treatment. *Chemosphere*, *308*, 136312.

Jarollahi, R., & others. (2023). Magnetic properties of Fe_3O_4 nanoparticles with controlled size and morphology. *Journal of Magnetism and Magnetic Materials*, *565*, 170313.

Khlyustova, A., Sirotkin, N., Kusova, T., Kraev, A., Titov, V., & Agafonov, A. (2020). Doped TiO_2: The effect of doping elements on photocatalytic activity. *Materials Advances*, *1*(5), 1193–1201.

Kubiak, A. (2023). Phase transition of TiO_2 and its impact on dielectric constant. *Materials Chemistry and Physics*, *299*, 127426.

Kustiningsih, W., and others. (2022). The potential of iron sand as a raw material for the functional materials industry in Indonesia. *Proceedings of the National Seminar on Materials*, 112–118.

Limbong, A. (2013). Polarization distribution in PVDF and its copolymer P(VDF/TrFE) near the surface. *Indonesian Journal of Material Science*, 29–34.

Lubis, R., & Daulay, H. (2025). Study of the relationship between composition and functional properties of metal oxide ceramics. *Journal of Materials Science*, *18*(1), 25–34.

Lumban Toruan, P. L. T., Margareta, B., Jumarni, A., Pratiwi, S. S., & Atina, A. (2023). The effect of water temperature on conductivity and total dissolved solids. *Journal of Coil Physics*, *6*(1), 11–16.

Pap, Z., Baia, L., & Dombi, A. (2025). Photocatalytic degradation of paracetamol using TiO_2–Fe_3O_4 composites under UV irradiation. *Catalysts*, *15*(2), 221.

Pranata, I., Wulandari, F., & Siregar, R. (2022). Analysis of the resistance of ceramic composites in dry and wet conditions. *Journal of Materials Technology*, *13*(3), 187–196.

Prasetyo, A., & Pradistia, L. (2022). Analysis of PZT toxicity and lead-free material alternatives. *Indonesian Journal of Materials Science*, *20*(1), 44–53.

Riani, D. (2023). The effect of milling and sintering temperature on ceramic clay. *Journal of Physics Unand*, *12*(1), 15–23.

Rizky, D., Santoso, B., & Amalia, H. (2023). A simple method of testing the piezoelectric properties of ceramics uses a multimeter. *Journal of Electronics and Functional Materials*, *5*(2), 77–84.

Roscow, I., Topolov, V. Y., & Bowen, C. R. (2016). Understanding the peculiarities of the piezoelectric effect in macro-porous $BaTiO_3$. *Journal of Physics D: Applied Physics*, *49*(37)

J. Phys.: Theor. Appl. Vol. 10 No. 1 (2026) 36-43 doi: 10.20961/jphystheor-appl.v10i1.114433

Shen, Y. (2025). Development status of textured piezoelectric ceramics for lead-free energy applications. *Coatings*, *15*(1), 51.

Sutisna, H., and others. (2023). Production and application of TiO_2 in Indonesian industry. *Journal of Materials Technology*, *17*(4), 199–206.

Waruwu, et,al. (2023). Analysis of the effect of saline water and ringer lactate infusion solutions on the corrosion rate of Ti6Al-4V titanium alloys used for bone implants. *Journal of Mechanical Engineering*, *11*(4), 179–186.

Yotthuan, S., Suriwong, T., Pinitsoontorn, S., & Bongkarn, T. (2018). Effect of Fe_2O_3 doping on phase formation, microstructure, electric and magnetic propertiesof $(Ba_{0.85}Ca_{0.15})(Ti_{0.90}Zr_{0.10})O_3$ ceramics. *Integrated Ferroelectrics*, *187*(1), 100–112.